SLAC-PUB-11523

Contributed to 32nd International Conference on High-Energy Physics (ICHEP 04), 08/16/2004--8/22/2004, Beijing, China

PENTAQUARK SEARCHES AND PROPERTIES OF D_{sJ}RESONANCES AT *BABAR*

V. HALYO, REPRESENTING THE *BABAR* COLLABORATION

SLAC, SLAC M/S 61, 2575 Sand Hill Road, Menlo Park, CA 94025

E-mail: valerieh@slac.stanford.edu

Prelimary results from inclusive searches for strange pentaquark production in e^+e^- interactions at $\sqrt{s} = 10.58$ GeV using 123 fb^{-1} of data collected with the *BABAR* detector are presented. In addition new mass estimates for the $D^*_{sJ}(2317)^+$ and $D_{sJ}(2460)^+$ mesons are given. The mesons are studied in $e^+e^- \to c\bar{c}$ data using 125 fb^{-1} for the decay to the D_s^+ meson along with one or more π^0, π^+, or γ particles. A search is also performed for neutral and doubly-charged partners.

1 Introduction

Recently, several experimental groups have reported observations of new, manifestly exotic narrow baryon resonances [1,2,3,4,5,6,7] and discoveries of two new narrow mesons containing c and s quarks— the $D^*_{sJ}(2317)^+$ meson [8,9,10,11], and the $D_{sJ}(2460)^+$ meson, [9,10]. These new results reawakened interest in the study of QCD spectroscopy.

Here we present new studies using data collected with the *BABAR* detector[13] at the PEP-II asymmetric e^+e^- collider, operating at the $\Upsilon(4S)$ resonance and at a center-of-mass (CM) energy ~ 40 MeV below it. Detailed discussions of the topics in this paper may be found in the conference submissions [16,14,15]. All results are preliminary.

2 The D_s^+ Candidate

All of the final states explored in the charmed meson analysis involve one D_s^+ candidate decaying to $K^+K^-\pi^+$. Backgrounds are further suppressed by selecting decays to $\overline{K}^{*0}K^+$ and $\phi\pi^+$ [8]. Combinations of $K^-K^+\pi^+$ with $1.954 < m(K^+K^-\pi^+) < 1.981$ GeV/c^2 are taken as D_s^+ candidates.

Details of the fitting procedure corresponding to $D^*_{sJ}(2317)^+$ and $D_{sJ}(2460)^+$ mass measurements, including proper handling of reflections, are given in the conference submission[16]. In addition, the $D_s^+\pi^\pm$ invariant mass spectra were examined: no evidence of any narrow structure is found close to the $D^*_{sJ}(2317)$ mass. This is consistent with the $D^*_{sJ}(2317)$ being an isosinglet state.

3 The $D^*_{sJ}(2317)^+$ Mass

Estimates of the mass of the $D^*_{sJ}(2317)^+$ are obtained using a unbinned likelihood fit of the $D_s^+\pi^0$ mass spectrum. The background to the $D^*_{sJ}(2317)^+$ comes from unrelated D_s^+ and π^0 and from two types of reflections. One reflection, from $D_s^*(2112)^+ \to D_s^+\gamma$ decays combined with an unassociated γ to form a fake π^0 candidate, is peaked near the kinematic limit in $D_s^+\pi^0$ mass of 2154.6 MeV/c^2. The second reflection is produced by the D_s^+ and π^0 mesons from $D_{sJ}(2460)^+ \to D_s^*(2112)^+\pi^0$ decay. Due to a kinematic coincidence, this reflection has a mean mass that is close to the $D^*_{sJ}(2317)^+$ mass and because of the variation in reconstruction efficiency across the $D_{sJ}(2460)^+$ phase space, the reflection shape is asymmetric therefore it must be accurately determined in order to correctly measure the $D^*_{sJ}(2317)^+$ properties. The likelihood fit to the $D_s^+\pi^0$ mass spectrum results in preliminary measurement of the $D^*_{sJ}(2317)^+$ mass is $[2318.9 \pm 0.3\,(\text{stat.}) \pm 0.9\,(\text{syst.})]$ MeV/c^2.

Work supported in part by Department of Energy contract DE-AC02-76SF00515
SLAC, Stanford University, Stanford, CA 94309

Table 1. Preliminary measurements of the $D_{sJ}(2460)^+$ obtained from $D_s^+\gamma$, $D_s^+\pi^0\gamma$, and $D_s^+\pi^+\pi^-$ decays. The results, in units of MeV/c^2

$m(D_{sJ}(2460)^+ \to D_s^+\gamma) =$	2457.2 ± 1.6 (stat.) ± 1.3 (syst.)
$m(D_{sJ}(2460)^+ \to D_s^+\pi^0\gamma) =$	2459.1 ± 1.3 (stat.) ± 1.2 (syst.)
$m(D_{sJ}(2460)^+ \to D_s^+\pi^+\pi^-) =$	2460.1 ± 0.3 (stat.) ± 1.2 (syst.)

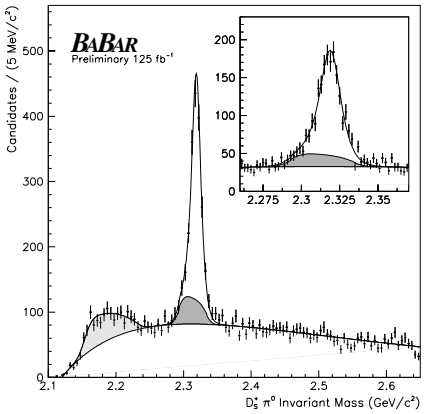

Figure 1. The $D_s^+\pi^0$ invariant mass distribution. The solid curve is the result of an unbinned likelihood fit. The dark (light) gray region is the contribution from the $D_{sJ}(2460)^+ \to D_s^+\pi^0\gamma$ ($D_s^*(2112)^+ \to D_s^+\gamma$) reflection. The inset is an expanded view near the $D_{sJ}^*(2317)^+$ mass.

4 The $D_{sJ}(2460)^+$ Mass

Estimates of the mass of the $D_{sJ}(2460)^+$ are obtained using an unbinned likelihood fit to the $D_s^+\gamma$, $D_s^+\pi^0\gamma$ and the $D_s^+\pi^+\pi^-$ systems. The likelihood fit to the $D_s^+\gamma$ system uses a signal lineshape determined from signal Monte Carlo. To determine the $D_{sJ}(2460)^+$ mass, the mean value of the signal is allowed to shift. To determine the mass from the $D_s^+\pi^0\gamma$ system additional issues that need to be addressed since it is a three body decay, In particular, it is reasonable to assume that the $D_{sJ}(2460)^+$ decays to $D_s^+\pi^0\gamma$ through either of two possible intermediate resonances: $D_s^*(2112)^+\pi^0$ or $D_{sJ}^*(2317)^+\gamma$. There is no *a priori* reason to favor one decay path over another. To invistigate any source of peaking background under the $D_{sJ}(2460)^+$ two $D_s^*(2112)^+$ sidebands were considered in $D_s^+\gamma$ mass The $D_s^+\pi^0\gamma$ mass distribution in these sidebands is included in Fig. 2. An important reflection appears from $D_{sJ}^*(2317)^+ \to D_s^+\pi^0$ decays combined with unassociated γ particles. Independent likelihood fits are applied to each of the sideband distributions and to the signal distribution. All three fits can successfully model their respective data samples, as shown in Fig. 2. The $D_{sJ}(2460)^+$ mass is included in the fit by allowing the lineshape to vary in mass. The likelihood fit to the $D_s^+\pi^+\pi^-$ mass distribution consists of three signal distributions ($D_{sJ}^*(2317)^+$, $D_{sJ}(2460)^+$, or $D_{s1}(2536)^+$ decay) plus a third-order polynomial to describe the combinatorial background. The shapes of the three signals are derived from signal Monte Carlo samples. The $D_{sJ}(2460)^+$ and $D_{s1}(2536)^+$ signal shapes are allowed to shift upwards and downwards in mass in order to best describe the data. The mass of the $D_{sJ}(2460)^+$ and $D_{s1}(2536)^+$ are obtained from this fit.

5 Θ_5^+, Ξ_5^{--} and Ξ_5^0 Searches

We reconstruct Θ_5^+ candidates in the pK_S^0 decay mode, where $K_S^0 \to \pi^-\pi^+$, with selection criteria based on geometrical and kinematic cuts designed for high efficiency and low bias against any production mechanism. The simulated signal reconstruction efficiency varies with p^*, the pK_S^0 momentum in the e^+e^- c.m. frame, from 13% at low p^* to 22% at high p^*. The invariant mass distribution of pK_S^0 is shown in Fig. 3. There is a clear peak at 2285 MeV/c^2 from $\Lambda_c^+ \to pK_S^0$ but no other sharp structure. We next search

Table 2. The upper limits at the 95% C.L. on the Θ_5^+ (Ξ_5^{--}) total production cross section times its branching fraction B, assuming a mass of 1540(1862) MeV/c^2 and two values of the natural width in MeV/c^2 $B\times$the number of Ξ_5^{--} produced per $e^+e^- \to q\bar{q}$ event and $B\times$the number per $\Upsilon(4S)$ decay.

particle	X-section U.L. (fb)		$q\bar{q}$ event U.L. (10^{-5}/event)		$\Upsilon(4S)$ decay U.L. (10^{-5}/event)	
	$\Gamma = 1$	$\Gamma = 8(18)$	$\Gamma = 1$	$\Gamma = 8(18)$	$\Gamma = 1$	$\Gamma = 8(18)$
Θ_5^+	182.8	363.1	5.39	10.71	17.90	34.98
Ξ_5^{--}	11.0	16.85	0.32	0.5	1.06	1.60

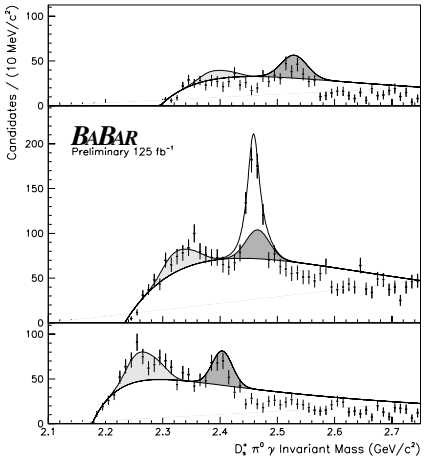

Figure 2. The $D_s^+\pi^0\gamma$ mass spectrum of the sample of events that fall in a $D_s^+\gamma$ signal region (center plot), the $D_s^+\gamma$ high mass sideband (top plot), and the low mass sideband (bottom plot). The $D_{sJ}(2460)^+$ signal appears only in the signal region. The results of separate likelihood fits are superimposed on all three distributions. Reflections from (dark gray) $D_{sJ}^*(2317)^+ \to D_s^+\pi^0$ and (light gray) $D_s^*(2112)^+ \to D_s^+\gamma$ decays appear in all three distributions at positions that are fixed from kinematics. The relative contribution of the $D_{sJ}^*(2317)^+$ reflection in each sample has been determined using signal Monte Carlo.

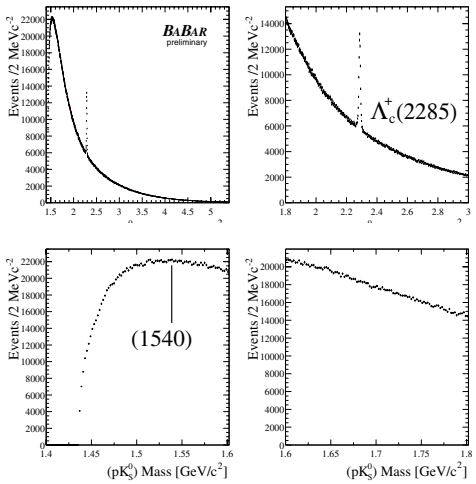

Figure 3. Distribution of the pK_S^0 invariant mass for combinations satisfying all the criteria described in the text. The same data are plotted four times in different pK_S^0 mass regions.

for the reported $\Xi_5^{--}(1862)$ and $\Xi_5^0(1862)$ states decaying into a Ξ^- and a charged pion, where $\Xi^- \to \Lambda^0\pi^-$ and $\Lambda^0 \to p\pi^-$,. The unique topology of this decay allows considerable background reduction by reconstructing the two displaced vertices and cutting around the Λ^0 and Ξ^- masses. The simulated signal reconstruction efficiency varies from 6.5% at low p^* to 12% at high p^*. The invariant mass distributions for $\Xi^-\pi^-$ and $\Xi^-\pi^+$ are shown in Fig. 4. For $\Xi^-\pi^+$ there are clear peaks as expected for the $\Xi^{*0}(1530)$ and $\Xi_c^0(2470)$ baryons, but no other structure is visible. For $\Xi^-\pi^-$, there is no visible sharp structure at all. Upper limits at the 95% C.L. on the

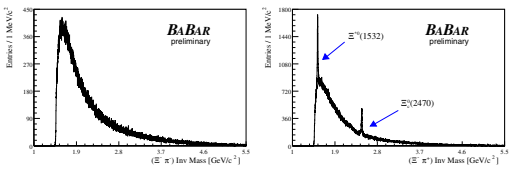

Figure 4. $\Xi^-\pi^-$ invariant mass distribution and $\Xi^-\pi^+$ invariant mass distribution.

Θ_5^+ (Ξ_5^{--}) production cross section times its branching fraction, are therefore calculated in a model independent way and given in ta-

ble 2

6 Conclusions

We find no evidence for the production of Θ_5^+ (1540), Ξ_5^{--} (1862) or any other member of the multiplet decaying to $\Lambda^0 K$ or $\Sigma^0 K$ final states in 123 fb^{-1}of *BABAR* data. Taking the upper limit widths, we calculate 95% C.L. upper limits on the total production rates of 1.1×10^{-4} Θ_5^+ and 1.0×10^{-5} Ξ_5^{--} per $e^+e^- \to q\bar{q}$ event (preliminary); these are roughly a factor of eight and four below the typical values measured for ordinary octet and decuplet baryons of the same masses as illustrated in Fig. 5. We also find no evidence for Θ^{*++} pentaquark in the decay $B^+ \to \Theta^{*++}\bar{p}$ where $\Theta^{*++} \to pK^+$ performed using 81 fb^{-1} of data. The upper limit on the branching fraction of $B^+ \to \Theta^{*++}\bar{p}$ of 1.5×10^{-7} for $1.43 < m(\Theta^{*++}) < 1.85\,\mathrm{GeV/c^2}$ [15]. Based on

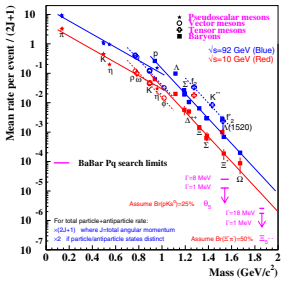

Figure 5. Compilation of baryon production rates in e^+e^- annihilation from experiments at the Z^0 (circles) and $\sqrt{s} \approx 10$ GeV (squares) as a function of baryon mass. The vertical scale accounts for the number of spin and particle+antiparticle states. The arrows indicate our preliminary upper limits on spin-1/2 Θ_5^+ and Ξ_5^{--} pentaquark states, assuming the branching fractions shown, and are seen to lie below the solid line.

125 fb^{-1} of $e^+e^- \to c\bar{c}$ data, the $D_{sJ}^*(2317)^+$ and $D_{sJ}(2460)^+$ masses are measured to be $[2318.9 \pm 0.3\,(\mathrm{stat.}) \pm 0.9\,(\mathrm{syst.})]$ MeV/c^2 and $[2459.4 \pm 0.3\ (\mathrm{stat.}) \pm 1.0\ (\mathrm{syst.})]$ MeV/c^2, respectively. And the fit to the $D_s^+\pi^+\pi^-$ mass spectrum also provides a preliminary estimate of the $D_{s1}(2536)^+$ mass: $[m(D_{s1}(2536)^+) = 2534.3 \pm 0.4\ (\mathrm{stat.}) \pm 1.2\ (\mathrm{syst.})]$ MeV/c^2. Searches for a neutral or doubly-charged partner for the $D_{sJ}^*(2317)^+$ decaying to $D_s^+\pi^+$ or $D_s^+\pi^-$ also produce no significant signal.

References

1. LEPS Collaboration, T. Nakano *et al.*, Phys. Rev. Lett. **91**, 012002 (2003).
2. SAPHIR Collaboration, J. Barth *et al.*, Phys. Lett. **B 572**, 127 (2003).
3. CLAS Collaboration, V. Kubarovsky *et al.*, Phys. Rev. Lett. **92**, 032001 (2004). Erratum; ibid, 049902.
4. DIANA Collaboration, V.V. Barmin *et al.*, Phys. Atom. Nucl. **66**, 1715 (2003).
5. HERMES Collaboration, A. Airapetian *et al.*, Phys. Lett. **B 585**, 213 (2004).
6. COSY-TOF Collaboration, M. Abdel-Bary *et al.*, Phys. Lett. **B 595**, 127 (2004).
7. NA49 Collaboration, C. Alt *et al.*, Phys. Rev. Lett. **92**, 042003 (2004).
8. *BABAR* Collaboration, B. Aubert *et al.*, Phys. Rev. Lett. **90**, 242001 (2003).
9. CLEO Collaboration, D. Besson *et al.*, Phys. Rev. **D68**, 032002 (2003).
10. BELLE Collaboration, K. Abe *et al.*, Phys. Rev. Lett. **92**, 012002 (2004).
11. BELLE Collaboration, P. Krokovny *et al.*, Phys. Rev. Lett. **91**, 262002 (2003).
12. *BABAR* Collaboration, B. Aubert *et al.*, Phys. Rev. **D69**, 031101 (2004).
13. The *BABAR* Collaboration, B. Aubert *et al.*, Nucl. Instrum. Methods **A479**, 1-116 (2002).
14. *BABAR* Collaboration, B. Aubert *et al.*, hep-ex/0408064.
15. *BABAR* Collaboration, B. Aubert *et al.*, hep-ex/0408037.
16. *BABAR* Collaboration, B. Aubert *et al.*, ICHEP 2004 abstract 10-0631, hep-ex/0408067.